Electronic Supplementary Material (ESI) for RSC Applied Polymers.

ELECTRONIC SUPPLEMENTARY INFORMATION

Aromatic Polypeptide Amphiphiles for Drug Adsorption: A New Approach for Drug Overdose Treatment

Karoline E. Eckhart,†[a] Hunter B. Wood,†[a] Tarik A. Taoufik,†[a] Michelle E. Wolf,[a] Dazhe J. Cao,[b] and Stefanie A. Sydlik*[a]

[a] Department of Chemistry, Carnegie Mellon University, 4400 Fifth Avenue, Pittsburgh, PA, USA

[b] Department of Emergency Medicine, University of Texas Southwestern Medical Center, Dallas, TX, USA

† These authors contributed equally

* Corresponding author – Email: ssydlik@andrew.cmu.edu

ABBREVIATIONS

Lys, lysine; K, lysine; Glu, glutamic acid; E, glutamic acid; Tyr, tyrosine; Y, tyrosine; NCA, α-amino acid N-carboxyanhydride; N_2, nitrogen gas; THF, tetrahydrofuran; $NaHCO_3$, sodium bicarbonate; HCl, hydrochloric acid; TLC, thin layer chromatography; $MgSO_4$, magnesium sulfate; DMSO, dimethyl sulfoxide; ^{1}H NMR, proton nuclear magnetic resonance; DMF, dimethylformamide; TFA, trifluoroacetic acid; HBr, hydrobromic acid; FTIR, Fourier transform infrared; AY3, acid yellow 3; ATL, amitriptyline; AC, activated charcoal; SGF, simulated gastric fluid; SIF, simulated intestinal fluid; PBS, phosphate-buffered saline; C_{free}, concentration of free adsorbate in the supernatant; C_o, initial concentration of adsorbate; C_{ads}, concentration of adsorbed adsorbent; % Ads, percent of adsorbate adsorbed; Q_e, adsorption capacity; Q_m, maxiumum adsorption capacity; K_L, Langmuir constant; σ_{est}, standard error of estimate; N, sample size; GPC, gel permeation chromatography;

SYNTHESIS OF NCA MONOMERS

Synthesis of Lys(Z)-NCA. H-Lys(Z)-OH (2.20 g, 7.85 mmol, 1 eq) was added to an oven-dried flask and high vacuum was applied overnight to evaporate adsorbed moisture. The flask was refilled with dry N_2 and the amino acid was dispersed dry THF to give a 0.1 M solution. Triphosgene (1.16 g, 3.92 mmol, 0.5 eq) was added in one shot under constant N_2 flow. The reaction mixture was reacted at 50 ˚C for 5 h. The reaction mixture was then evaporated to dryness to give a beige solid. The solid was redissolved in ethyl acetate, then consecutively washed with a mixture of 5% $NaHCO_3$ and ice (2 X 50 mL), 5% HCl and ice (2 X 50 mL), and brine with no ice (1 X 50 mL). TLC was used to confirm the presence of Lys(Z)-NCA in the organic layer (R_f = 0.47, 100% ethyl acetate). The organic layer was then dried over $MgSO_4$ and evaporated to a

concentrate. The concentrate was filtered through a silica plug into a flame-dried round bottom flask, and the plug was rinsed with ~100 mL of ethyl acetate. The solution was evaporated to a concentrate, put on ice, and hexanes was slowly added to precipitate the NCA. The precipitated NCA was vacuum filtered to give a white powder (1.98 g, 82% yield) which was stored at 4 ˚C. The structure and purity of Lys(Z)-NCA were confirmed by ^{1}H-NMR (500 MHz) in DMSO-d_6 (Figure S2).

Synthesis of Glu(OBzl)-NCA. H-Glu(OBzl)-OH (2.00 g, 8.43 mmol, 1 eq) was added to an oven-dried flask and high vacuum was applied overnight to evaporate adsorbed moisture. The flask was refilled with dry N_2 and the amino acid was dispersed in dry THF to give a 0.1 M solution. Triphosgene (1.25 g, 4.21 mmol, 0.5 eq) was added in one shot under constant N_2 flow. The reaction mixture was reacted at 50 ˚C for 3 h. The reaction mixture was then evaporated to dryness to give a pale yellow solid. The solid was redissolved in ethyl acetate, then consecutively washed with a mixture of 5% $NaHCO_3$ and ice (2 X 50 mL), 5% HCl and ice (2 X 50 mL), and brine with no ice (1 X 50 mL). TLC was used to confirm the presence of Glu(OBzl)-NCA in the organic layer (R_f = 0.59, 100% ethyl acetate). The organic layer was then dried over $MgSO_4$ and evaporated to a concentrate. The concentrate was filtered through a silica plug into a flame-dried round bottom flask, and the plug was rinsed with ~100 mL of ethyl acetate. The solution was evaporated to a concentrate, put on ice, and hexanes was slowly added to precipitate the NCA. The precipitated NCA was vacuum filtered to give a white powder (1.85 g, 83% yield) which was stored at 4 ˚C. The structure and purity of Glu(OBzl)-NCA were confirmed by ^{1}H-NMR (500 MHz) in DMSO-d_6 (Figure S3).

Synthesis of Tyr(OBzl)-NCA. H-Tyr(OBzl)-OH (2.40 g, 8.85 mmol, 1 eq) was added to an oven-dried flask and high vacuum was applied overnight to evaporate adsorbed moisture. The flask was

refilled with dry N_2 and the amino acid was dispersed in dry THF to give a 0.1 M solution. Triphosgene (1.31 g, 4.42 mmol, 0.5 eq) was added in one shot under constant N_2 flow. The reaction mixture was reacted at 50 ˚C for 5 hours. The reaction mixture was then evaporated to dryness to give a green-white solid. The solid was redissolved in ethyl acetate, then consecutively washed with a mixture of 5% $NaHCO_3$ and ice (2 X 50 mL), 5% HCl and ice (2 X 50 mL), and brine with no ice (1 X 50 mL). TLC was used to confirm the presence of Tyr(OBzl)-NCA in the organic layer (R_f = 0.44, 100% ethyl acetate). The organic layer was then dried over $MgSO_4$ and evaporated to a concentrate. The concentrate was filtered through a silica plug into a flame-dried round bottom flask, and the plug was rinsed with ~100 mL of ethyl acetate. The solution was evaporated to a concentrate, put on ice, and hexanes was slowly added to precipitate the NCA. The precipitated NCA was vacuum filtered to give a white powder (2.27 g, 86% yield) which was stored at 4 ˚C. The structure and purity and Tyr(OBzl)-NCA were confirmed by ^{1}H-NMR (500 MHz) in DMSO-d_6 (Figure S4).

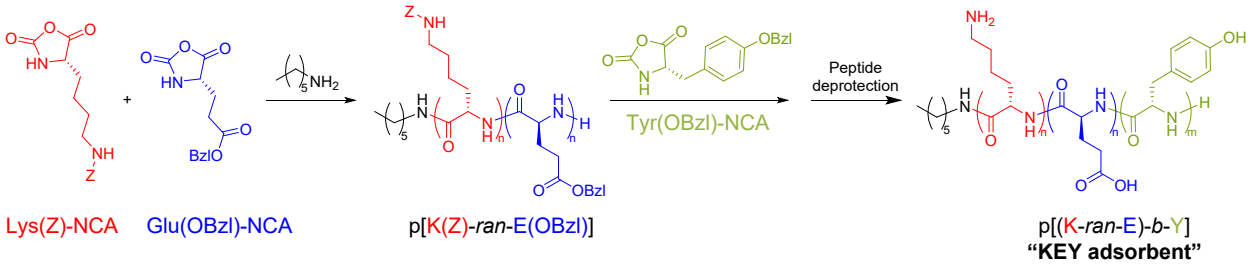

Scheme S1. Synthesis of KEY polypeptide adsorbents.

Synthesis of p[K(Z)-ran-E(OBzl)] macroinitiator. Lys(Z)-NCA (1.7460 g, 5.7 mmol, 20 eq) and Glu(OBzl)-NCA (1.5005 g, 5.7 mmol, 20 eq) were added to an oven-dried flask, vacuum-backfilled thrice with dry N_2, and dissolved in dry dimethylformamide (DMF) to give a 0.45 M solution. Then, hexylamine (0.285 mmol, 1 eq) was added from a solution in dry DMF, where the concentration of the hexylamine solution was accurately known by quantitative NMR. The polymerization was stirred under N_2 for 5 min, then a light vacuum (ca. 300 mBar) was applied for 10 min. Next, the polymerization was stirred under a static vacuum until complete consumption of the comonomers was observed by ^{1}H-NMR (approximately 4 h). The resulting p[K(Z)-*ran*-E(OBzl)] was used as a macroinitiator in the synthesis of p[(K(Z)-*ran*-E(OBzl))-*b*-Y(OBzl)], described in the next section. The remaining p[K(Z)-*ran*-E(OBzl)] was precipitated with ice cold diethyl ether and centrifuged at 2420 × *g* for 10 min to pellet the copolypeptide, resulting in a white powder that was stored at room temperature (Figure 6a).

Synthesis of p[(K(Z)-ran-E(OBzl))-b-Y(OBzl)]. Three separate p[(K(Z)-*ran*-E(OBzl))-*b*-Y(OBzl)] copolypeptides were synthesized with varying equivalents of Tyr(OBzl)-NCA (10 eq, 20 eq, 30 eq) with respect to p[K(Z)-*ran*-E(OBzl)] macroinitiator. The same p[K(Z)-*ran*-E(OBzl)] macroinitiator was used for the synthesis of all KEYs. In general, the appropriate amount of Tyr(OBzl)-NCA was added to an oven-dried round bottom flask, vacuum-backfilled thrice with

N_2, and dissolved in dry DMF to give a 0.45 M solution. Next, p[K(Z)-ran-E(OBzl)] (1 eq) was added to the Tyr(OBzl)-NCA solution while stirring under dry N_2. The polymerization was stirred at room temperature for 3 days under static vacuum, as described above. Following complete consumption of the monomer, the reaction solution was precipitated in either methanol or diethyl ether on ice and centrifuged at 2420 × *g* for 10 min to pellet the copolypeptide. The copolypeptide was redissolved in DMF and precipitated again in either methanol or diethyl ether, resulting in a white powder that was stored at room temperature (Figure 7a).

Copolypeptide deprotection. In a typical copolypeptide deprotection, the protected copolypeptide (1 g) was dissolved in TFA (10 mL) and glacial acetic acid (3.3 mL). Then, 6.6 mL of HBr (48% in water) was added to the flask, resulting in the appearance of a thick white precipitate that redissolved over time. The reaction mixture was stirred at room temperature overnight. The reaction was then evaporated to a concentrate and precipitated into tetrahydrofuran (8x the volume of the concentrated copolypeptide solution) while vigorously stirring on ice. The copolypeptide, a white solid, was collected via centrifugation, dispersed in deionized water, and dialyzed against deionized water for 4 days using SnakeSkin™ dialysis tubing with a 3500 molecular weight cutoff. Following dialysis, the deprotected copolypeptide was lyophilized to dryness to give a fluffy, white powder and stored at room temperature. Successful deprotection of the KEY polypeptides was demonstrated by ^{1}H NMR and FTIR spectroscopy (Figures S6b, S7b, and S8).

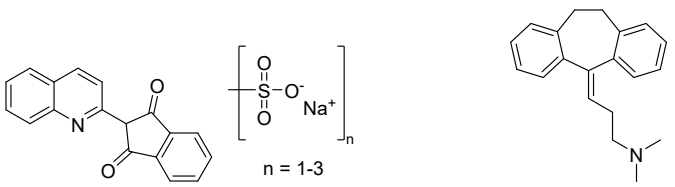

Acid yellow 3 Amitriptyline

Figure S1. Chemical structure of model adsorbates, acid yellow 3 (AY3) and amitriptyline (ATL).

General procedure for adsorption experiments. Adsorption experiments (both adsorption kinetics and adsorption capacity) were performed according to the following general procedure. Here, the KEYs and AC are termed "adsorbents;" acid yellow 3 and amitriptyline are termed "adsorbates;" and the buffer was either SGF, SIF or PBS. Stock solutions of adsorbate (500 μg/mL) and adsorbent (1 mg/mL) were accurately prepared in buffer and stored at -20 °C. All adsorbates were readily soluble in buffer. Adsorbents were insoluble but could be homogeneously dispersed by vortexing. In a typical adsorption experiment, a known volume of adsorbent dispersion was combined in a 1.5 mL Eppendorf tube with a known volume of adsorbate stock solution, giving a mixture with a final volume of 450 μL. For each condition tested, the concentration of the adsorbate in the final mixture was calculated using the known concentration of the adsorbent stock, volume of adsorbent stock, and volume of the final mixture; whereas the initial concentration of free adsorbate (C_o) was determined experimentally with a control experiment where the adsorbate stock solution was combined with a blank buffer (containing no adsorbate). The Eppendorf was vortexed briefly to mix, then incubated at 37 °C (MyTemp Mini Digital Incubator, Benchmark Scientific) with rotational shaking (MiniMixer^{TM}, Benchmark Scientific). After a designated incubation period, the Eppendorf was centrifuged at 10,000 × g for 10 min (Centrifuge 5418, Eppendorf) to pellet the adsorbent. Next, a 100 μL aliquot (containing the free adsorbate) was

siphoned from the supernatant of the tube, being careful not to disturb the pellet, and the aliquot was dispensed into a 96 well plate. Each supernatant was plated thrice (3 x 100 µL). The absorbance of the supernatant was then analyzed using a plate reader, allowing determination of the concentration of free adsorbate in the supernatant (C_{free}, µg/mL) using the linear regression of calibration curves (ESI, Figure S10 for calibration curves). Using this and the experimentally determined initial concentration of adsorbate (C_o), Equations S1 – S3 were used to calculate the concentration of adsorbed adsorbent (C_{ads}, µg/mL), the percent of adsorbate adsorbed (% Ads), and the adsorption capacity (Q_e, mg adsorbent adsorbed per g adsorbent).

$$C_{ads} = C_o - C_{free} \quad \textbf{Equation S1}$$

$$\%\, Ads = 100 \times \frac{C_{ads}}{C_o} \quad \textbf{Equation S2}$$

$$Q_e = \frac{C_{ads}}{concentration\ of\ adsorbent} \quad \textbf{Equation S3}$$

Non-linear isotherm fitting. To determine Q_m and K_L values from the adsorption capacity experiments, the experimental data set ($Q_{e,exp}$ versus C_e) was fit to the non-linear form of the Langmuir isotherm equation (Equation 1). Using estimated Q_m and K_L values and experimental C_e values, a theoretical set of Q_e values ($Q_{e,calc}$) was calculated. X^2 was calculated to quantify the deviation between the $Q_{e,calc}$ values and experimental Q_e ($Q_{e,exp}$) values according to Equation 3. Next, using the Solver add-in in Microsoft Excel, the estimated Q_m and K_L values were optimized until a minimum value of X^2 was reached. Error bars for the Q_m values displayed in Figure 6 are the standard error of the estimate (σ_{est}), as determined by Equation S4, where N is the sample size of experimental determinations.

$$\sigma_{est} = \sqrt{\frac{\sum (Q_{e,calc} - Q_{e,exp})^2}{N-2}} \quad \textbf{Equation S4}$$

MATERIAL CHARACTERIZATION METHODS

KEY polypeptide adsorbents were characterized to determine degree of deprotection (FTIR and ^{1}H NMR), amino acid composition (^{1}H NMR), and dispersity (GPC).

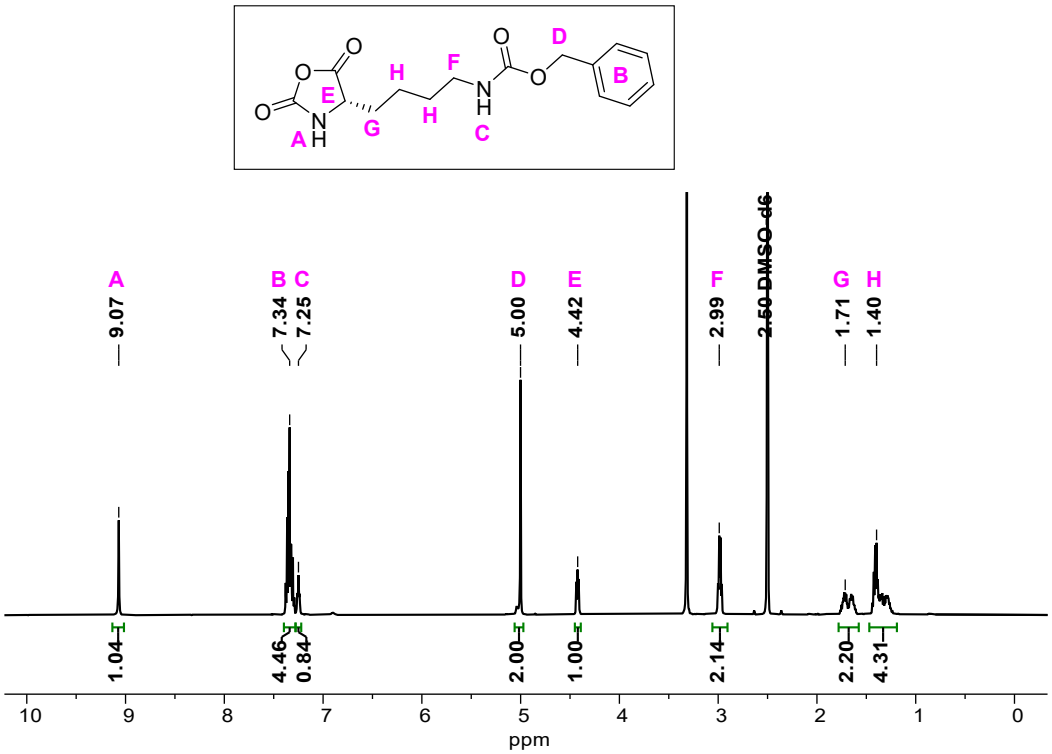

Figure S2. ^{1}H-NMR of Lys(Z)-NCA in DMSO-d^{6}.

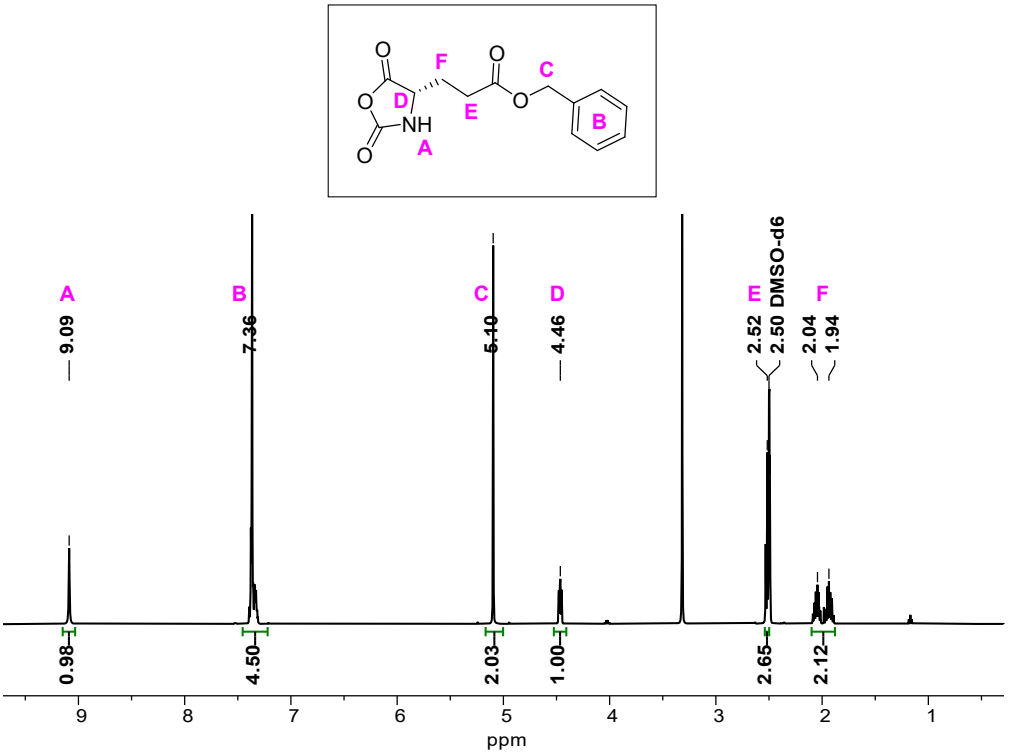

Figure S3. ^{1}H-NMR of Glu(OBzl)-NCA in DMSO-d^{6}.

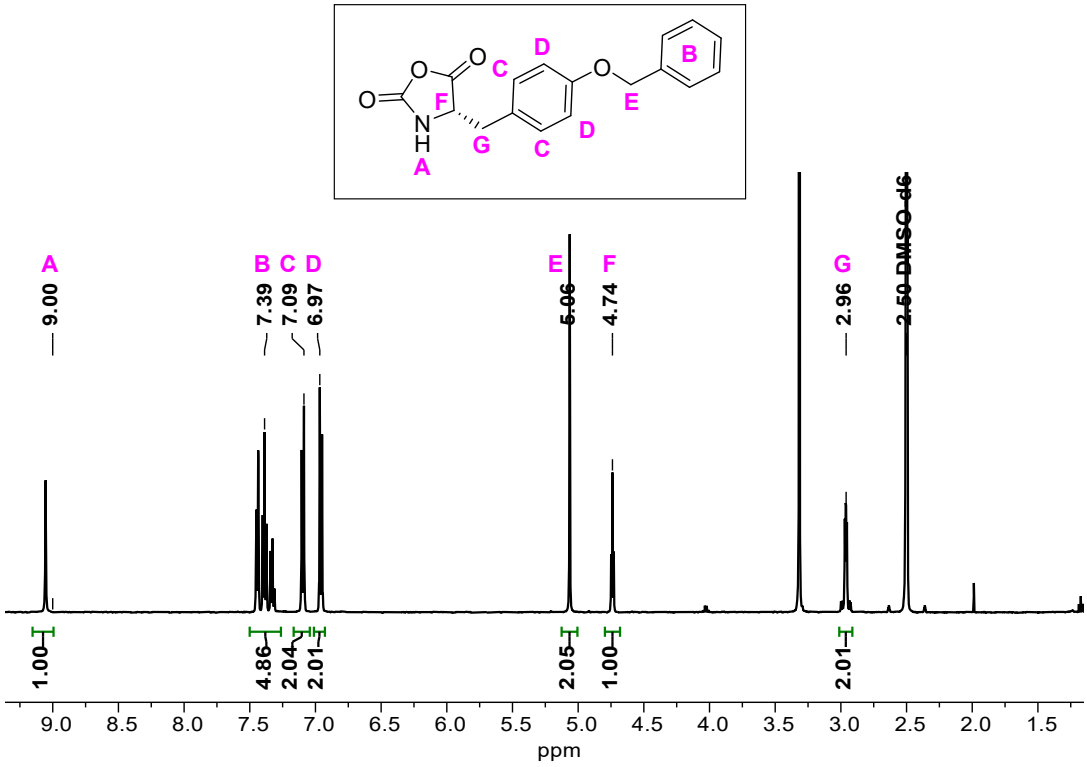

Figure S4. ^{1}H-NMR of Tyr(OBzl)-NCA in DMSO-d^{6}.

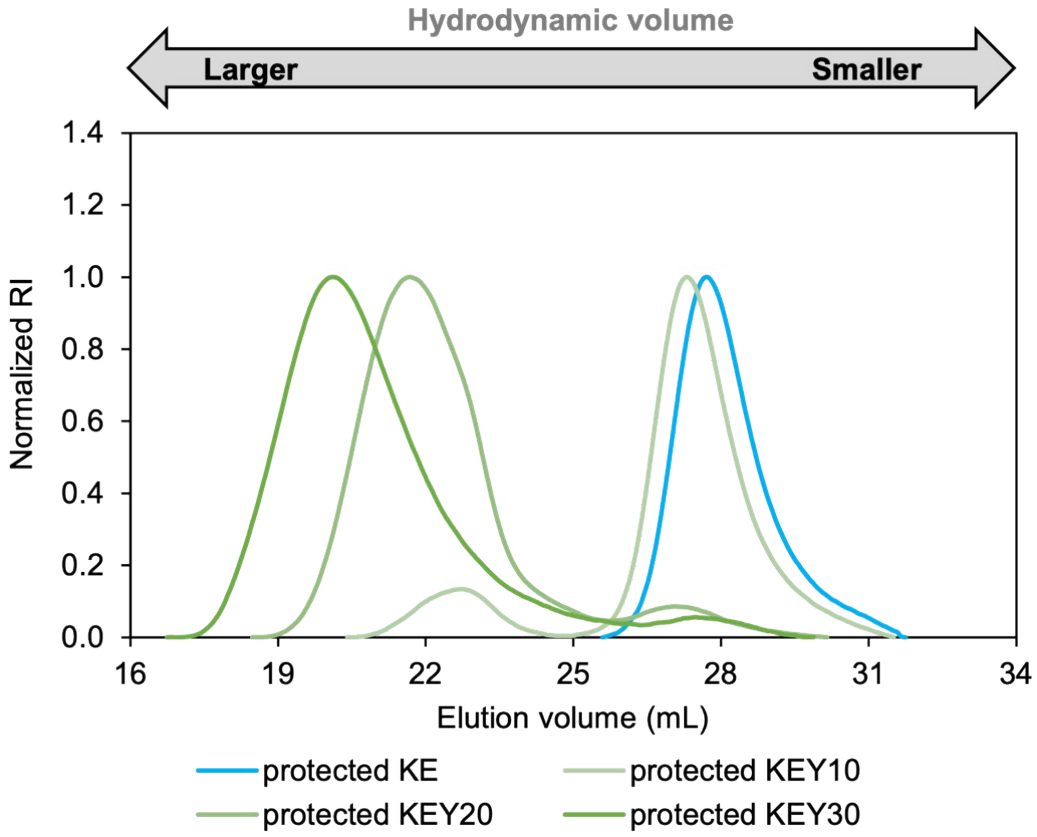

Figure S5. Gel permeation chromatography of protected KEYs in dimethylformamide for dispersity determinations. Signals at low elution volume (16-25 mL) represent polypeptide aggregates. Signals at high elution volume (25-32 mL) represent the molecular weight distribution of the polypeptide which is below the secondary structure transition.

The amino acid composition of the KE macroinitiator was determined by ^{1}H-NMR end group analysis. Degree of deprotection is calculated for the KE macroinitiator from the protecting group aromatic protons according to the following equation:

$$\frac{\#\ deprotected\ aromatic\ protons}{\#\ protecting\ aromatic\ protons}\ x\ 100\%$$

The amino acid composition of the KEY polypeptide was determined in the same manner as the KE macroinitiator. When determining degree of deprotection for KEY polypeptides, aromatic protons that are contributed from tyrosine residues must be accounted for in the calculation. KEY formulations (KEY10, 20 and 30) appear similar by ^{1}H NMR; the major difference is reflected only in changes to the integral values, depending on the length of the tyrosine block. Spectra for the KE macroinitiator and a representative KEY formulation (KEY20) are given below.

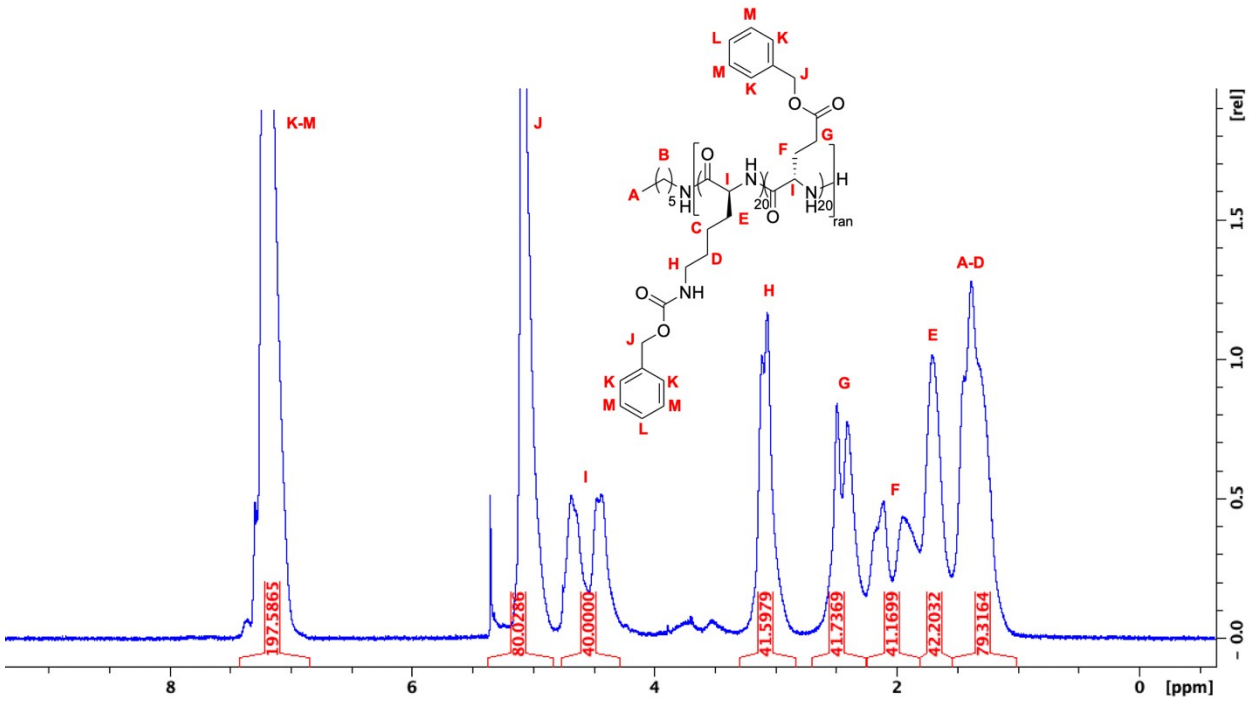
K-M
J
I
H
G
F
E
A-D
197.5865
80.0286
40.0000
41.5979
41.7369
41.1699
42.2032
79.3164
[rel]
[ppm]

(a)

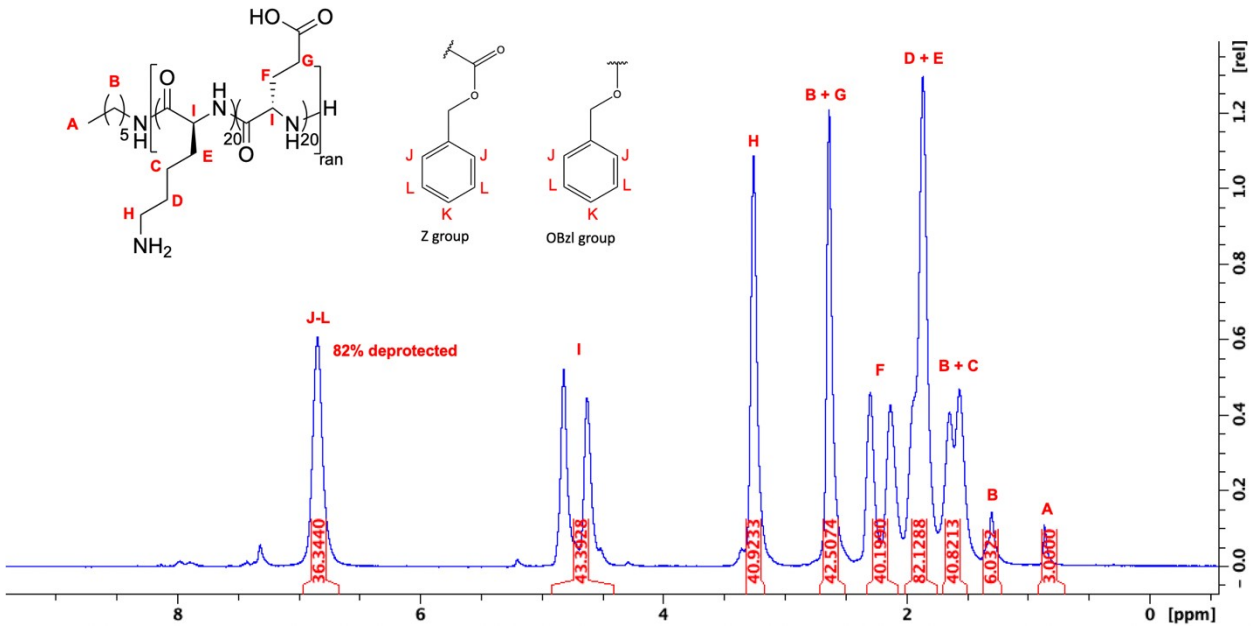
Z group
OBzl group
J-L
82% deprotected
I
H
B + G
D + E
F
B + C
B
A
36.3440
43.3928
40.9233
42.5074
40.1940
82.1288
40.8213
6.0322
3.0000
[rel]
[ppm]

(b)

Figure S6. ^{1}H-NMR quantitation of (a) protected and (b) deprotected K20E20 macroinitiator in TFA-d. In (a), intermolecular forces (i.e. π-stacking) can cause slower tumbling of molecules which results in lower resolution.

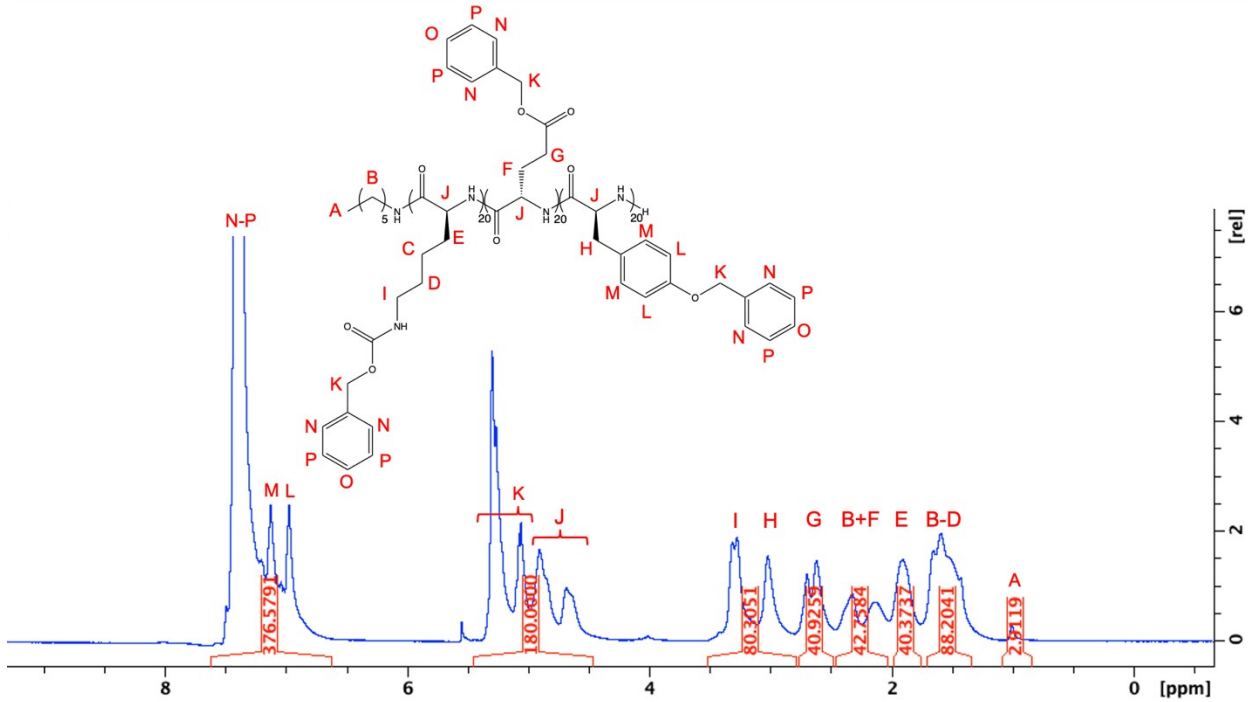

(a)

(b)

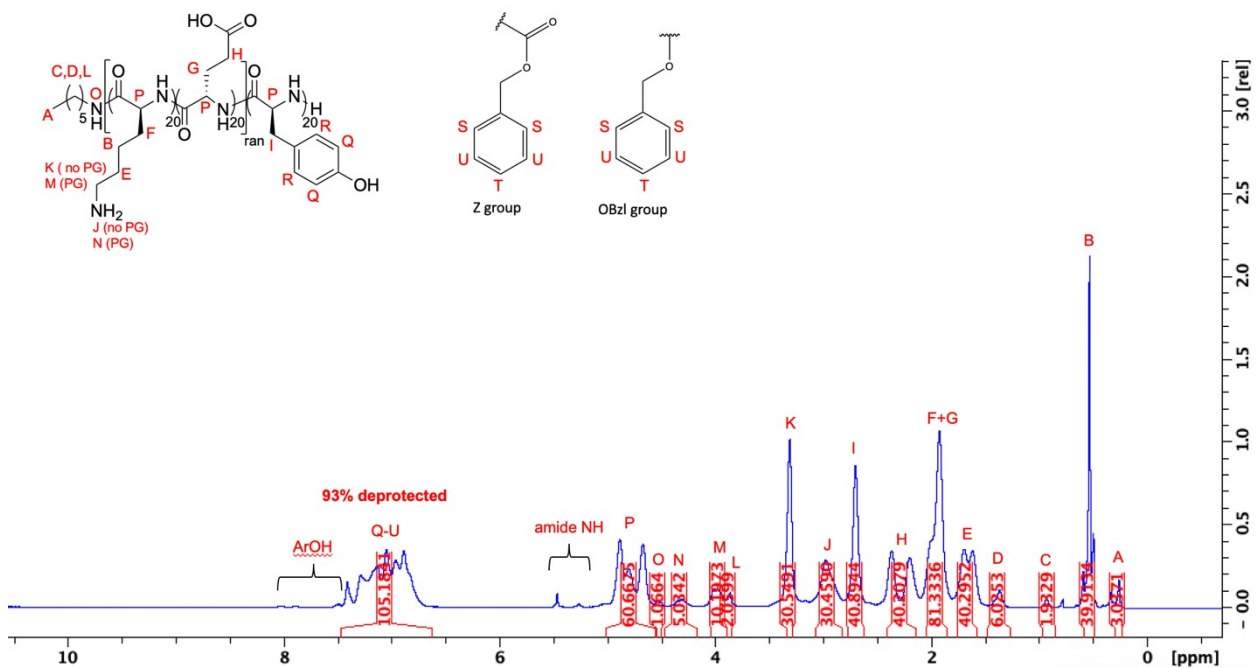

Figure S7. ^{1}H-NMR quantitation of (a) protected KEY20 polypeptide and (b) deprotected KEY20 polypeptide in TFA-d. In (a), intermolecular forces (i.e. π-stacking) can cause slower tumbling of molecules which results in lower resolution.

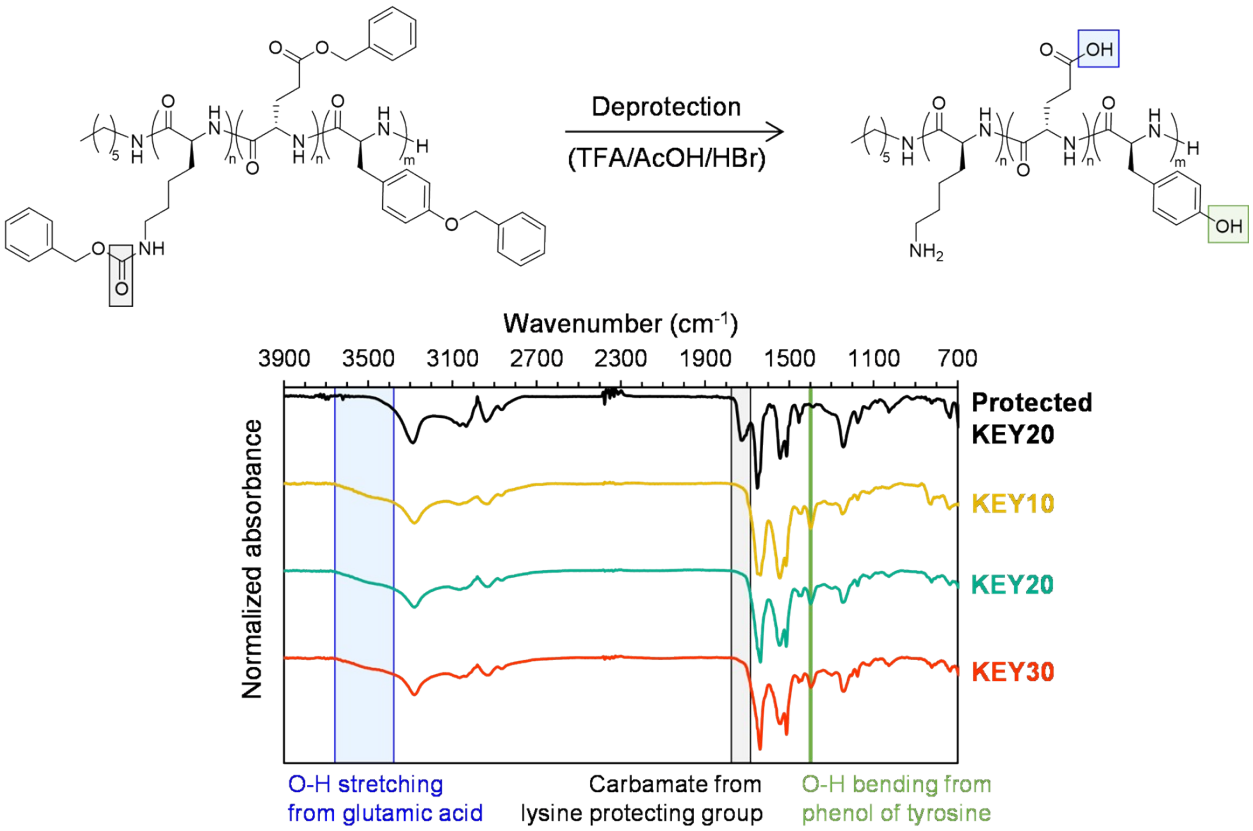

Figure S8. FTIR comparing the protected versus deprotected KEYs indicates successful deprotection. Complete deprotection of the lysine residues is evidenced by the disappearance of the carbamate peak at 1724 cm^{-1}. Successful deprotection of the glutamic acid and tyrosine residues is evidenced by the appearance of O-H stretching (3430 cm^{-1}) and O-H bending (1398 cm^{-1}) peaks, respectively.

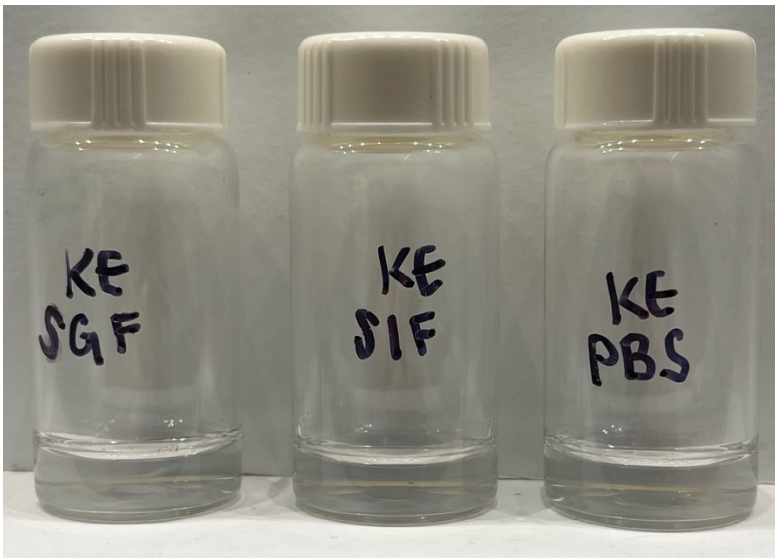

Figure S9. Photograph of poly[(lysine)$_{20}$-ran-(glutamic acid)$_{20}$] (poly(KE)) dissolved at 1 mg/mL in media. Because it lacks a tyrosine block, poly(KE) is completely soluble in SGF, SIF, and PBS.

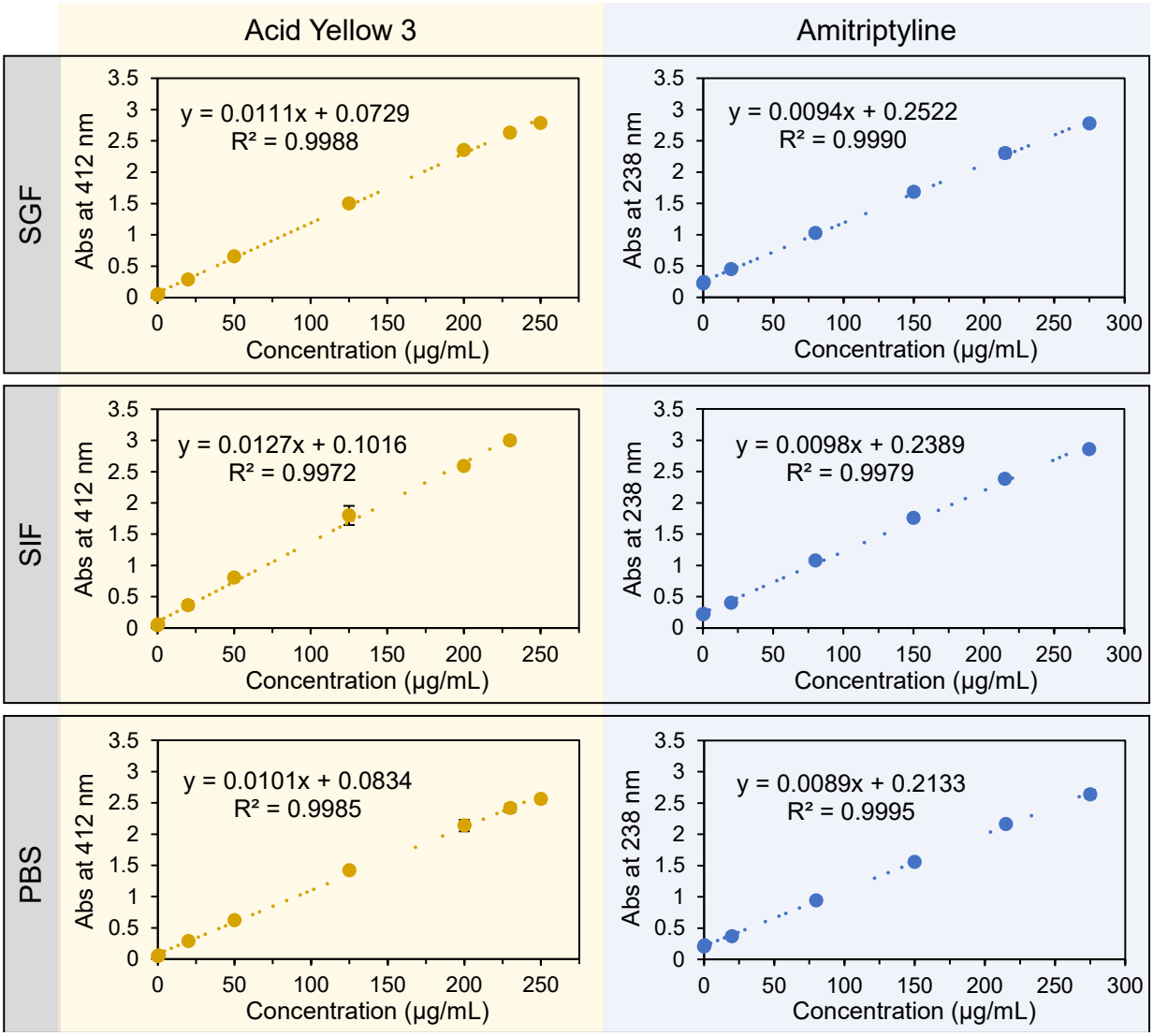

Figure S10. Calibration curves of adsorbates (Acid Yellow 3 and Amitriptyline) in simulated gastric fluid (SGF), simulated intestinal fluid (SIF), and phosphate buffered saline (PBS).

Figure S11. Results of control study used to validate the presence of electrostatic interactions. Adsorption of AY3 by KEY20 was evaluated in SGF under elevated salt concentration (left; 20 mg/mL additional NaCl) and under standard conditions (right). The vial on the left was visibly more yellow and demonstrated higher absorbance by UV-Vis spectroscopy, indicating that intermolecular interactions are present in the mechanism of adsorption of AY3 to KEYs.

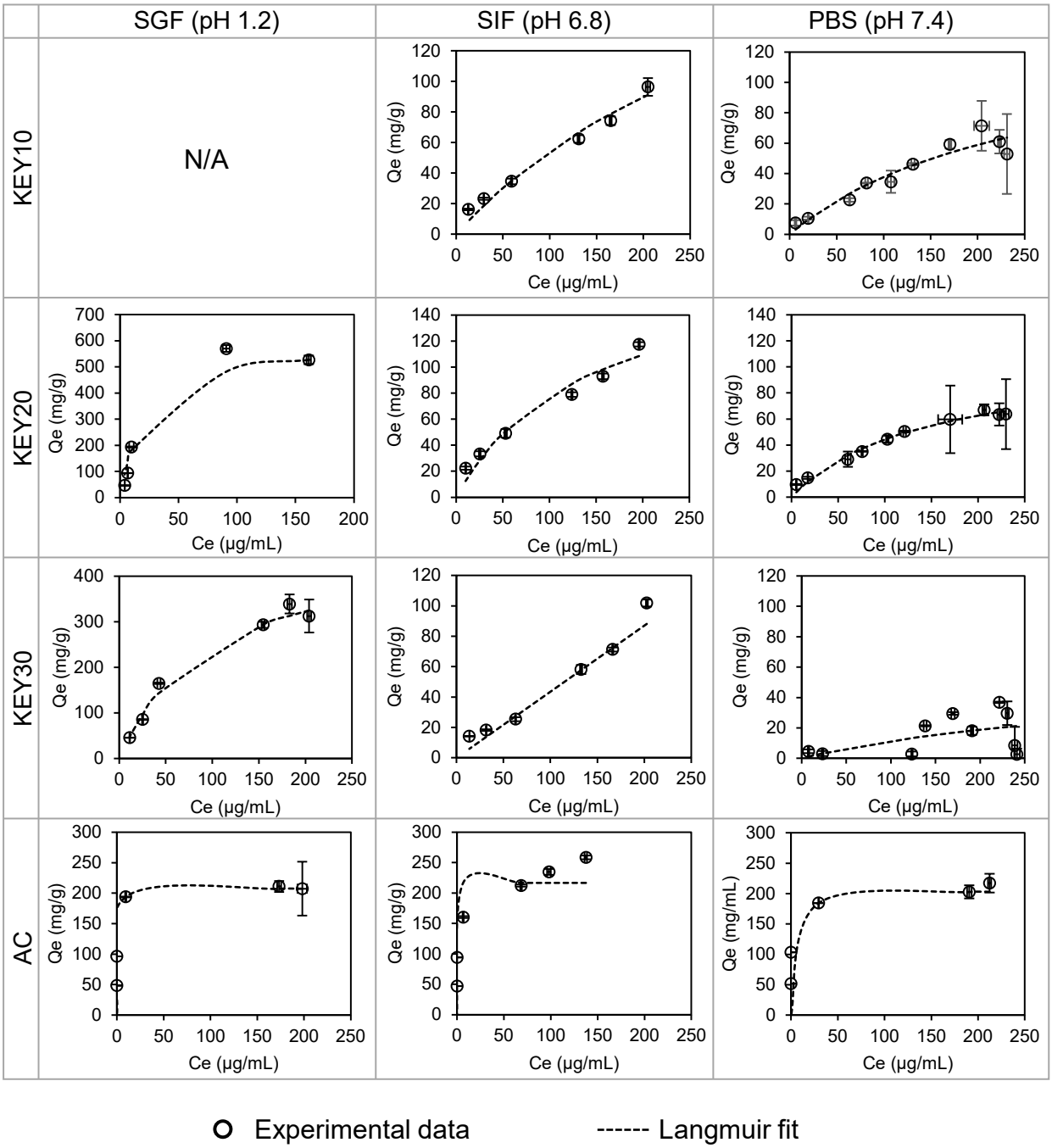

Figure S12. Adsorption of acid yellow 3 (AY3) by the KEYs and AC was fit to the non-linear Langmuir isotherm model.

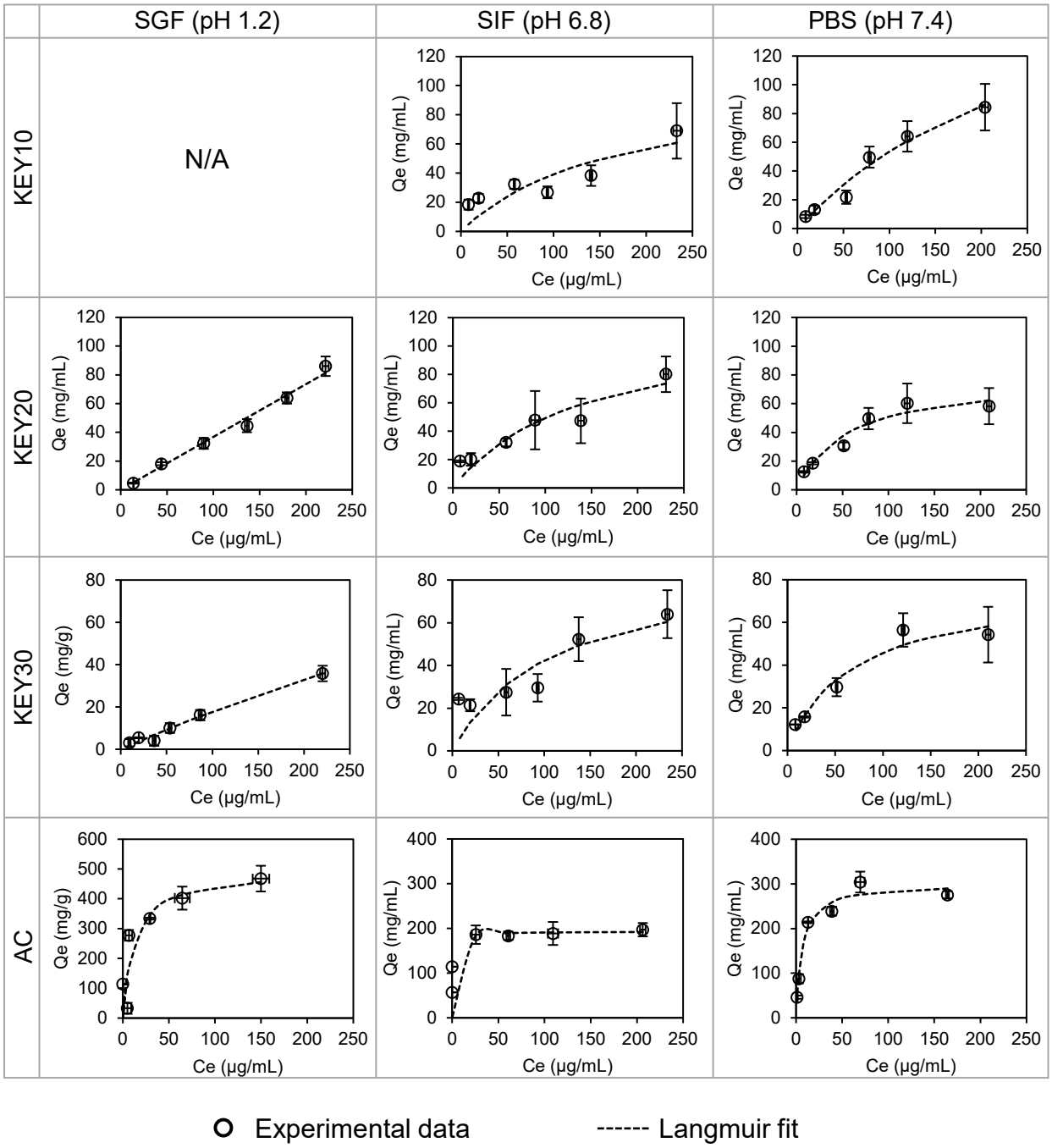

Figure S13. Adsorption of amitriptyline (ATL) by the KEYs and AC was fit to the non-linear Langmuir isotherm model.

Table S1. Summary of "goodness of fits" of the experimental adsorption data to the Langmuir linear and non-linear models.

	KEY10	KEY20	KEY30	AC
AY3 / SGF	Adsorbent is soluble	R^2 = 0.953 χ^2 = 48.1	R^2 = 0.965 χ^2 = 6.6	R^2 = 0.973 χ^2 = 0.10
ATL / SGF	Adsorbent is soluble	Experimental data did not fit linear OR nonlinear Langmuir models.	R^2 = 0.707 χ^2 = 2.8	R^2 = 0.992 χ^2 = 4,865.8
AY3 / SIF	R^2 = 0.810 χ^2 = 8.9	R^2 = 0.288 χ^2 = 10.9	Experimental data did not fit linear OR nonlinear Langmuir models.	R^2 = 0.990 χ^2 = 24.2
ATL / SIF	R^2 = 0.715 χ^2 = 59.0	R^2 = 0.762 χ^2 = 30.5	R^2 = 0.732 χ^2 = 70.2	R^2 = 0.999 χ^2 = 0.4
AY3 / PBS	R^2 = 0.644 χ^2 = 12.3	R^2 = 0.864 χ^2 = 10.9	Experimental data did not fit linear OR nonlinear Langmuir models.	R^2 = 0.998 χ^2 = 1.0
ATL / PBS	R^2 = 0.961 χ^2 = 4.3	R^2 = 0.957 χ^2 = 2.6	R^2 = 0.960 χ^2 = 3.5	R^2 = 0.995 χ^2 = 7.5

The goodness of fit of the experimental data to the Langmuir isotherm was evaluated using R^2 (for linear fitting) and χ^2 (for non-linear fitting). An R^2 approaching 1 represents a good fit for the linear Langmuir model. A low χ^2 represents a good fit for the non-linear Langmuir model.

Table S2. Comparison of results determined by fitting experimental adsorption data to the non-linear and linearized forms of the Langmuir equation.

Full agreement	Partial agreement	Not in agreement	Poor fit to linear & nonlinear forms

	KEY10	KEY20	KEY30	AC
AY3 / SGF	N/A (Adsorbent is soluble)	Q_m and K_L of nonlinear and linear models are in agreement.	Q_m and K_L of nonlinear and linear models are in agreement.	Q_m is in agreement. K_L of linear form is negative.
ATL / SGF	N/A (Adsorbent is soluble)	Experimental data did not fit the linear OR nonlinear Langmuir models.	Q_m and K_L are NOT in agreement. Error in nonlinear values is lower than error in linear values.	Q_m is in agreement. K_L of linear is 64% higher than K_L of nonlinear.
AY3 / SIF	Q_m and K_L are NOT in agreement. Error in nonlinear values is lower than error in linear values.	Q_m is in agreement. K_L of linear is 93% lower than KL of nonlinear.	Experimental data did not fit the linear OR nonlinear Langmuir models.	Q_m is in agreement. Only linear fit yields reasonable K_L value.
ATL / SIF	Q_m and K_L are NOT in agreement. Error in nonlinear values is lower than error in linear values.	Q_m is in agreement. K_L of linear is 56% higher than K_L of nonlinear	Q_m is in agreement. K_L of linear is 43% higher than K_L of nonlinear	Q_m is in agreement. K_L of linear is 120% lower than KL of nonlinear
AY3 / PBS	Q_m is in agreement. K_L of linear is 28% lower than K_L of nonlinear.	Q_m and K_L of nonlinear and linear models are in agreement.	Experimental data did not fit the linear OR nonlinear Langmuir models.	Q_m is in agreement. K_L of linear is 77% higher than K_L of nonlinear.
ATL / PBS	Q_m and K_L are NOT in agreement. Error in nonlinear values is lower than error in linear values.	Q_m and K_L of nonlinear and linear models are in agreement.	Q_m is in agreement. K_L of linear is 26% higher than K_L of nonlinear	Q_m is in agreement. K_L of linear is 27% higher than K_L of nonlinear

The Q_m and K_L values obtained by the non-linear and linearized Langmuir fits were compared, and the agreement of these values in each adsorbent-adsorbate-media condition was color-coded according to the legend above. Here, "in agreement" is defined as within standard error (for Q_m values) or less than 20% difference (for K_L values).

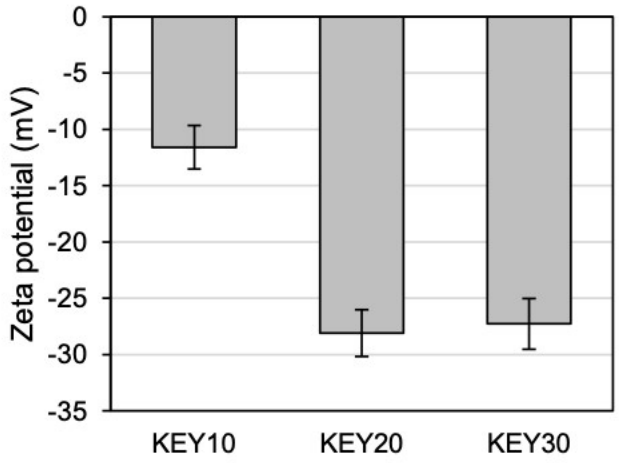

Figure S14. Zeta potentials of KEYs in deionized water buffered to pH 7 using 5% NaOH

REFERENCES

(1) Rey-Mafull, C. A.; Tacoronte, J. E.; Garcia, R.; Tobella, J.; Llópiz, J. C.; Iglesias, A.; Hotza, D. Comparative Study of the Adsorption of Acetaminophen on Activated Carbons in Simulated Gastric Fluid. *SpringerPlus* **2014**, *3* (1), 48. https://doi.org/10.1186/2193-1801-3-48.

(2) Stippler, E.; Kopp, S.; Dressman, J. B. Comparison of US Pharmacopeia Simulated Intestinal Fluid TS (without Pancreatin) and Phosphate Standard Buffer PH 6.8, TS of the International Pharmacopoeia with Respect to Their Use in In Vitro Dissolution Testing. *Dissolution Technol.* **2004**, *11* (2), 6–10.